# Modeling Dissolution of Sparingly Soluble Multisized Powders

LUÍS PEREIRA DE ALMEIDA[†], SÉRGIO SIMÕES[†], PAULO BRITO[‡], ANTÓNIO PORTUGAL[‡], AND MARGARIDA FIGUEIREDO[‡x]

Received October 8, 1996, from the [†]*Laboratório de Galénica e Tecnologia Farmacêutica, Faculdade de Farmácia, and* [‡]*Departamento de Engenharia Química, Faculdade de Ciências e Tecnologia, Universidade de Coimbra, 3000 Coimbra, Portugal.* Accepted for publication March 14, 1997[⊗].

**Abstract** ☐ The dissolution of powder drugs, besides being a topic of utmost importance, especially for the sparingly soluble ones, is far from being well-explained. The purpose of the present study is, on the one hand, to obtain experimental dissolution profiles and, on the other hand, to analyze and process the data for dissolution modeling. Three different size fractions of a widely used sparingly soluble drug—ibuprofen—were fully characterized with regard to its particle size distribution, specific surface area, density, solubility, and diffusion coefficient. The dissolution profiles were obtained making use of a technique that counts and sizes particles—the Coulter counter technique—which is capable of following the number and size of the particles in suspension throughout time. The knowledge of these parameters allowed a critical study of the assumptions associated with the models currently used to describe the dissolution process. It was concluded that most of the assumptions were not valid for the present experimental conditions. This motivated the proposal of a new methodology, which uses the experimentally determined characteristics of the drug and takes into account the polydisperse nature of the powder. By applying an adequate dissolution equation to each of the many size classes in which the primary particle size distribution was divided, it was possible to obtain a large agreement between the simulated and the experimental dissolution profile.

## Introduction

Dissolution tests of powdered drugs are currently used for drug characterization. Although they are mostly utilized as quality control methods (to ensure end product quality or batch to batch consistency), they may also be correlated to *in vivo* activity. In fact, it is now well-recognized that the rate of dissolution often controls the drug bioavailability, in particular for poorly soluble drugs where dissolution is the rate-limiting step. Numerous examples can be found in pharmaceutical literature illustrating the critical importance of dissolution kinetics on the extent and rate of drug absorption.[1,2] However, to manipulate the bioavailability of the administered drug, a full understanding of the dissolution phenomenon is crucial. Nevertheless, despite the proposal of various models to describe the release kinetics of sparingly soluble drugs,[3,4] no general agreement has yet been found to interpret dissolution data.

Earlier studies, undertaken to investigate the influence of particle size on the dissolution rate of indomethacin,[5,6] revealed that the classical dissolution models did not adequately explain the experimentally obtained dissolution profiles. These were fully discussed regarding their applicability and associated assumptions.

The emphasis of the present work is on the development of a mathematical procedure which takes into account the polydisperse nature of the powder and the variation of the particle number throughout dissolution, factors which have not been contemplated in the classical models. Furthermore, this method also intends to be applicable to distinct size ranges. For this, three different size fractions of ibuprofen were dissolution tested and the corresponding experimental dissolution profiles were compared with the simulated ones. All the steps of this procedure will be described in detail.

[⊗] Abstract published in *Advance ACS Abstracts,* May 1, 1997.

**Table 1—Classical Dissolution Models[a]**

| *h* | Integrated Equation | Rate Dissolution Constant | eq |
|---|---|---|---|
| constant | $w_0^{1/3} - w^{1/3} = K_{1/3}t$ | $K_{1/3} = \frac{1}{3}N^{1/3}\frac{D}{h}\pi\left(\frac{6}{\pi\rho}\right)^{2/3}C_S$ | (2) |
| *kd* | $w_0^{2/3} - w^{2/3} = K_{2/3}t$ | $K_{2/3} = \frac{2}{3}N^{2/3}\frac{D}{k}\pi\left(\frac{6}{\pi\rho}\right)^{1/3}C_S$ | (3) |
| $k\sqrt{d}$ | $w_0^{1/2} - w^{1/2} = K_{1/2}t$ | $K_{1/2} = \frac{1}{2}N^{1/2}\frac{D}{k}\pi\left(\frac{6}{\pi\rho}\right)^{1/2}C_S$ | (4) |

[a] $k$ = constant, $d$ = particle diameter, $N$= particle number, $w_0$ = suspended solids weight at time $t = 0$, and $w$ = suspended solids weight at time $t = t$.

## Theoretical

Many theoretical models have been proposed to characterize the dissolution mechanism of multiparticulate systems since the first equation presented by Noyes and Whitney in 1897.[7] Most models assume quasi-steady-state diffusion and are based on the following equation:[8,9]

$$\frac{dW}{dt} = \frac{D}{h}S(C_S - C) \qquad (1)$$

where $W$ = dissolved solids weight, $t$ = time, $D$ = diffusion coefficient, $h$ = diffusion layer thickness, $S$ = interfacial area, $C_S$ = solubility, and $C$ = dissolved concentration.

The so-called classical diffusional models result from the integration of eq 1 supposing that the diffusion coefficient is independent of concentration and time and the particle shape nearly spherical. Particle monodispersity is assumed and therefore the interfacial area is easily related to the solids weight ($S$ is proportional to $w^{2/3}$), considering a constant particle number. The fundamental differences between these models rely upon the interdependency between the diffusion layer thickness *(h)* and particle size (*d*). Indeed, while some authors, like Hixson and Crowell,[10] for example, assume *h* to be a constant, others considered *h* to be proportional to the particle diameter—approximately equal to the particle radius, like Higuchi and Hiestand,[11] or its square root, like Niebergall *et al.*[12] Different algebraic relations between *h* and *d* result, obviously, in different equations for the integrated form of eq 1. These equations, together with the associated assumptions regarding the value of *h* and the corresponding dissolution rate constants are presented in Table 1.

Despite the wide variation of the power to which *w* is raised (eqs 2−4), good agreements have been reported for either model. An explanation for this can probably be found in a more detailed analysis of the assumptions made for each model. For instance, it has been shown that eq 2 describes the dissolution kinetics of large particles well,[10] whereas, for the smaller ones, good agreements have been found using eq


*S0022-3549(96)00417-0 CCC: $14.00*

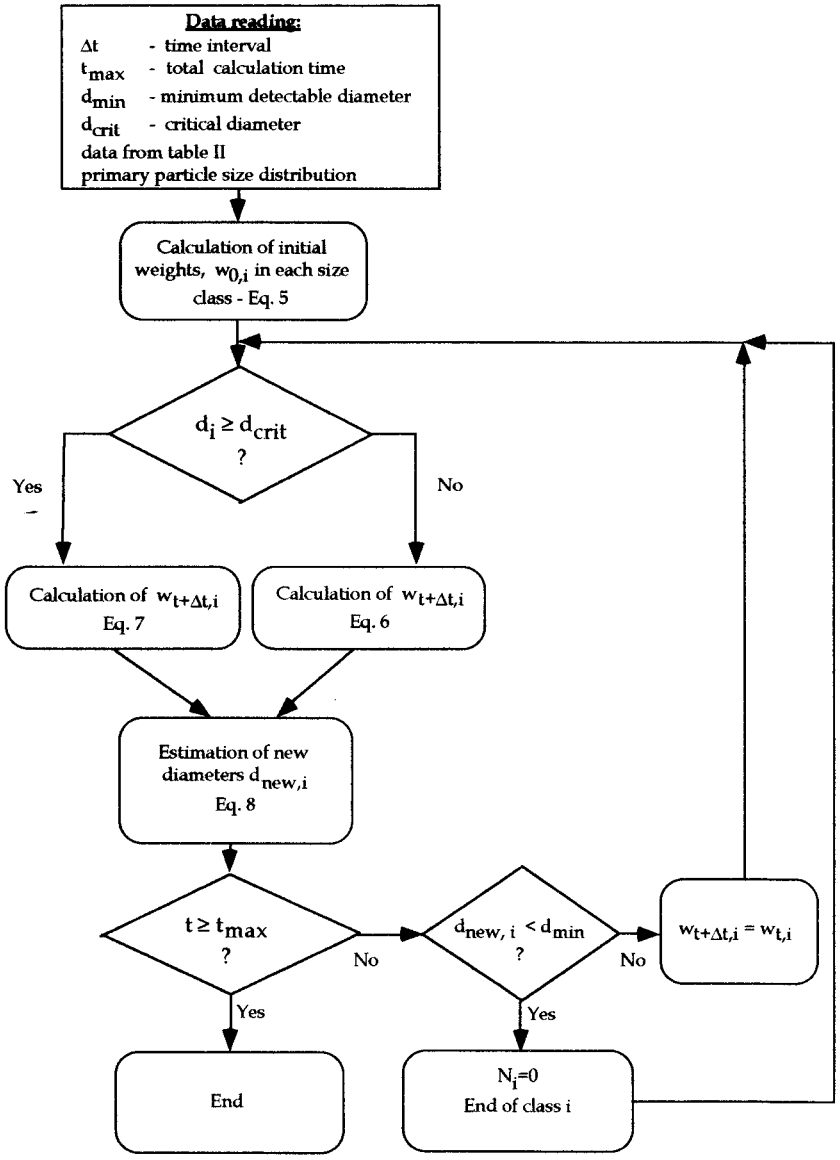


**Figure 1**—Flowchart of the program.

3.[11,13] Moreover, and especially for the fine particles, a size (and time) dependent diffusion layer thickness seems a more realistic approach than a constant value of *h* over the particle lifetime. However, Hintz and Johnson[14] and Lu *et al.*,[15] among other authors, postulate that *h* varies linearly with *d* up to a certain value, beyond which *h* remains unaltered. This assumption encompasses the differences in the release kinetics reported above for both small and large particles.

Nevertheless, in a previous work,[6] some of the present authors have shown that probably more important than the relationship between *h* and *d* is the validity of the other assumptions implicit in the models. Indeed, taking into account factors, like the change in the number of suspended particles throughout dissolution, their departure from sphericity, or the polydispersity degree, can result in a significant improvement in the model fitting. Some of these factors (although separately) have already been discussed by other authors.[11,16–18] However, most of these studies are mathematically complex and assume that the particle size distribution follows a log–normal law which, in many cases, represents an oversimplification.

The methodology adopted here intends to be generally applicable, i.e., valid for any particle size distribution following any dissolution equation, and, in addition, mathematically simple. It consists of dividing the primary particle size distribution into a large number of classes so that the particles in each size class could be considered monosized, in accordance with the assumptions of the dissolution models. Although the particle analyzer utilized (Coulter Multisizer II) can distribute the particles in 64, 128, and 256 size classes (channels), only 64 classes were used, since no improvements were detected in the fittings using a larger number of classes. In this way, significant computing time was saved. The next step was to choose between a size dependent on or independent of diffusion layer thickness, and the consequent dissolution equation. The first choice was to assume a linear relationship between *h* and *d* (eq 3). That had already been suggested in previous studies[6,19] and has more physical meaning. Nevertheless this model was not found to be adequate for the coarsest fraction, as will be described later. In this case, a better fit was achieved considering a constant value for *h*, above a certain particle size ($d_{crit}$). This is in agreement with the authors who suggest that *h* does not always increase with particle size but reaches a plateau at some critical value.[14,15]

With this in mind, a Fortran 77 program was written, the flowchart of which is presented in Figure 1. From the initial

data supplied by the Coulter Multisizer, which is basically the number of particles per size class ($N_i$), the weight of solids in each class is calculated according to

$$w_{0,i} = N_i \rho \frac{\pi d_i^3}{6} \tag{5}$$

where $N_i$ = number of particles in size class $i$, $\rho$ = solids density, $d_i$ = mean diameter of size class $i$, and $w_{0,i}$ = particles weight at time $t = 0$ for size class $i$.

It should be emphasized that the diameter given by the Coulter gives a volume-based diameter [$d_v = (6v/\pi)^{1/3}$, $v$ being the particle volume directly measured by the Coulter]. Hence, eq 5 is an accurate expression even for nonspherical particles.

Depending on $d_i$, the following dissolution equations were used to calculate the solids weight decrease

$$w_{t+\Delta t,i}^{2/3} = w_{t,i}^{2/3} - N_i^{2/3} K t \qquad \text{when } d_i < d_{\text{crit}} \tag{6}$$

$$K = \frac{2D}{3k} \alpha_{s,dv} \left(\frac{6}{\pi\rho}\right)^{1/3} C_S$$

and

$$w_{t+\Delta t,i}^{1/3} = w_{t,i}^{1/3} - N_i^{1/3} K t \qquad \text{when } d_i \geq d_{\text{crit}} \tag{7}$$

$$K = \frac{1}{3k} \frac{D}{d_{\text{crit}}} \alpha_{s,dv} \left(\frac{6}{\pi\rho}\right)^{2/3} C_S$$

where $w_{t+\Delta t,i}$ = suspended particles weight at time $t + \Delta t$ for size class $i$, $k$ = constant (see Table 1), $\alpha_{s,dv}$ = particle shape factor, and $d_{\text{crit}}$ = critical diameter.

It should be noted that eqs 6 and 7 are similar to eqs 3 and 2, respectively. The only difference is the experimental particle shape factor ($\alpha_{s,dv}$) used instead of $\pi$ (only valid for spheres).

The time interval utilized in the calculations ($\Delta t$) was small, typically 1 s, in order to ensure a constant $N_i$, which is another requirement of the classical models. After each time interval, a new value of $d_i$ was calculated according to

$$d_{\text{new},i} = \left(\frac{6 w_{t+\Delta t,i}}{\rho N_i \pi}\right)^{1/3} \tag{8}$$

Whenever $d_i$ became smaller than the minimum detectable by the Coulter, $d_{\text{min}}$ (±2% of the aperture tube), the particles in this class were considered completely dissolved. That leads, obviously, to a decrease in the overall particle number. A $t_{\text{max}}$ was user-defined and read as data.

The total weight of suspended solids can be estimated at any time value as the summation of the weights calculated for each size class. The dissolution profiles obtained in this way could then be compared to the experimental ones in order to optimize the values of $k$ (=$h/d$) and $d_{\text{crit}}$, as will be discussed in a subsequent section.

## Experimental Section

Ibuprofen was the drug selected for this study because it is a widely used NSAID that is sparingly soluble at low pH. Since one of the objectives was to test the applicability of the dissolution models to different size ranges, fractions of nominal sizes 25, 38, and 50 $\mu$m were utilized. These fractions, used as supplied, were fully characterized with respect to particle size distribution, solubility, diffusion coefficient, specific surface area, and density. Differential scanning calorimetry was also utilized to guarantee that all the fractions corresponded to the same racemic mixture of (+)- and (−)-enantiomers.

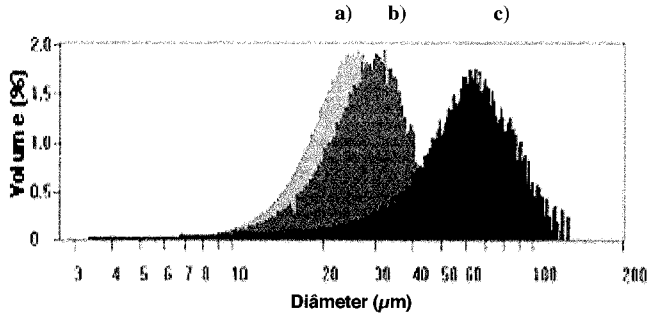


**Figure 2**—Primary particle size distribution measured by the Coulter Multisizer II for the ibuprofen fractions: (a) 25 $\mu$m, (b) 38 $\mu$m, and (c) 50 $\mu$m nominal size.

**Physical Characterization of Ibuprofen Fractions**—The primary particle size distribution of all fractions was determined using the Coulter Multisizer II. This apparatus counts and sizes particles suspended in an electrolyte according to the electrical sensing zone method.[20] This method is largely used in particle size characterization[21] and has recently been successfully applied to dissolution studies of pharmaceutical powders.[5,22] It provides dynamic information not only on the particle number and size distribution but also on the concentration of suspended solids, enabling the evaluation of dissolution profiles.

This technique requires a previous calibration of the apparatus, which is normally performed with latex spheres of known size. However, the primary calibration procedure recommends the use of the particles under analysis.[23] This procedure, often known as self-calibration, was the one followed in this work. Although more laborious than latex calibration, self-calibration is more accurate since it accounts for the particle properties (e.g. shape, conductivity, and porosity).[24]

In order to determine the primary size distribution, and in spite of the low solubility of ibuprofen, the particles were suspended in previously saturated drug solutions. A 100 $\mu$m aperture tube was employed for the experiments with the 25 and 38 $\mu$m fractions, while for the 50 $\mu$m fraction, a 200 $\mu$m tube was used. All the experiments were carried out at least four times.

In order to transform the weight of the particles in surface area, without assuming any specific particle shape, it is necessary to determine the particle shape factor, $\alpha_{s,dv}$.[20] This requires the knowledge of the powder specific surface area,[25] which in turn was estimated by the BET method in the ASAP 2000 from Micromeritics, using krypton as adsorbate.[26]

As the Coulter Multisizer output is given in terms of the volume of the solids and eq 1 utilizes the solids' weight, it is necessary to convert volume into weight (or mass) using for that the true density of the material. This was measured by helium pycnometry in the Accupyc from Micromeritics.[26]

The diffusion coefficient was evaluated using the rotating disk method.[27] Disks were prepared by compressing 300 mg of ibuprofen with a hydraulic press, in a 13 mm diameter die, applying a pressure of 1 ton during 1 min. The disks were inserted in a special device in which only one face is exposed to the solvent. The rotating speed was 100 rpm. During the dissolution process, the liquid was forced to pass through a spectrophotometer that automatically monitored the fluid absorbence.

The ibuprofen solubility was determined by spectrophotometric assay at 221 nm of ibuprofen saturated solutions. These were prepared by dispersing an ibuprofen excess of about 3 times the solubility on the dissolution medium.

Both the diffusion coefficient and the solubility measurements were performed in triplicate at 23 ± 1 °C.

**Experimental Dissolution Profiles**—As mentioned before, the Coulter Multisizer II enables the dissolution process to be monitored in terms of particle concentration. The amount of dissolved drug is calculated from the difference between the initial particle concentration and that remaining at any instant of time, as described in detail elsewhere.[5] The suspending medium was potassium dihydrogen phosphate buffer solution at pH = 4.5,[28] complemented with 0.01% Tween 80 to facilitate solids dispersion. All tests were repeated, under sink conditions, at least six times at room temperature (23 ± 1 °C).

**Table 2—Physical Characteristics of Ibuprofen Samples[a]**

| Fraction Nominal Size, $\mu$m | Volume Median Diameter ($d_{50}$), $\mu$m | Shape Factor ($\alpha_{s,dv}$) | Solubility ($C_s$), $\mu$g/mL | Diffusion Coefficient ($D$) $\times 10^6$ cm$^2$/s | Density ($\rho$) g/cm$^3$ |
|---|---|---|---|---|---|
| 25 | 22.9 ± 0.2 | 4.1 ± 0.1 | 73 ± 1.7 | 6.54 ± 0.04 | 1.11 ± 0.01 |
| 38 | 27.3 ± 0.4 | 3.6 ± 0.2 | 73 ± 1.3 | 6.65 ± 0.17 | 1.11 ± 0.01 |
| 50 | 52.6 ± 0.3 | 3.2 ± 0.1 | 71 ± 1.7 | 6.55 ± 0.08 | 1.11 ± 0.01 |

[a] Average values ± standard deviation.

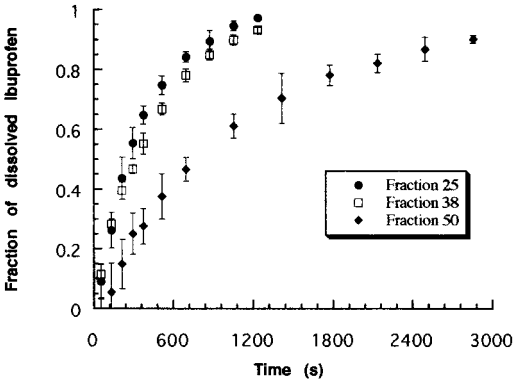


**Figure 3**—Dissolution profiles obtained with the Coulter Multisizer II. (Error bars represent the standard deviation of a mean of six experiments.)

## Results and Discussion

**Physical Characterization**—Figure 2 shows the primary size distribution of the three fractions of ibuprofen tested, measured by the Coulter Multisizer II. As can be seen, the fractions of nominal size 25 and 38 $\mu$m have very similar size distributions, in spite of the different nominal sizes specified by the supplier. The 50 $\mu$m fraction was found to be considerably coarser. Besides, and as will be more clearly shown in Figure 6, this fraction is much broader than the other two. The corresponding volume median diameters ($d_{50}$) are listed in Table 2 together with the remaining characteristics of the fractions determined, as described earlier. The values obtained for the diffusion coefficient, solubility, and density are approximately the same, regardless of the fraction size. On the contrary, a decrease in the shape factor ($\alpha_{s,dv}$) was noticed as the fraction size increased. This was, somehow, unexpected since the shape factor is normally size independent. However, the fractions tested (used as supplied) may not have been produced exactly in the same conditions and this could be responsible for the encountered differences in $\alpha_{s,dv}$.

**Dissolution Profiles**—The dissolution profiles are displayed in Figure 3 for the different ibuprofen fractions. As expected, a strong influence of the initial particle size was detected. The curves corresponding to the 25 and 38 $\mu$m fractions are approximately the same, most certainly due to the similarity of both size distributions. On the other hand, a much slower release was found for the coarsest fraction.

The dissolution data was treated according to eqs 2 and 3, and the results are presented in Figure 4. As this figure shows, no significant improvements were found by using different models. In fact, in both cases, a nonlinear tendency of the experimental profiles was observed, which is more noticeable for the coarsest fraction. As the two models only differ in the relationship between the diffusion layer thickness and particle size, it can be concluded that this is not, at least exclusively, the only reason for the lack of fitting. However, it should be remembered that these models have other implicit assumptions, namely particle sphericity, constant particle number throughout dissolution, and monodispersity. A careful examination of the validity of these assumptions led to the following conclusions:

(1) The experimentally determined shape factors (Table 2) indicate that the ibuprofen particles are not very far from spherical ($\alpha_{s,dv} = \pi$ for spheres), the lowest value corresponding to the coarsest fraction.

(2) As for the total particle number ($N$), Figure 5 shows that there is a continuous decrease of this parameter from the very beginning of dissolution, for all size fractions.

(3) As illustrated in Figure 6 and previously in Figure 2, the particles in each fraction are not monosized, fraction 50 being considerably broader than the remaining fractions. Furthermore, Figure 6 shows that, for example, the size distribution of fraction 50 is better approximated by a normal rather than by a log−normal distribution, frequently assumed by a number of authors.[11,15−18]

From these findings, it can be concluded that at least some of the model-associated assumptions are not fulfilled, which may explain the encountered discrepancies when trying to fit the classical models to the experimental data. Moreover, the higher deviations found for the coarsest fraction (Figure 4) are most certainly due to the broadness of its size distribution, confirming the need to account for this aspect.

As an attempt to overcome this problem, and as described in section 2, a methodology was developed which takes into account the change in particle number and the polydisperse nature of the powder. Additionally, it uses the real particle shape factor and does not require the particles to follow any specific size distribution law. A preliminary simulated dissolution profile was evaluated using the primary particle size distribution of fraction 25 and the parameters of Table 1. Equation 6 was the one selected with a value of $k = 0.5$ ($h$ is equal to the particle radius) as suggested by Higuchi and Hiestand.[11] Although a similar trend was obtained for the

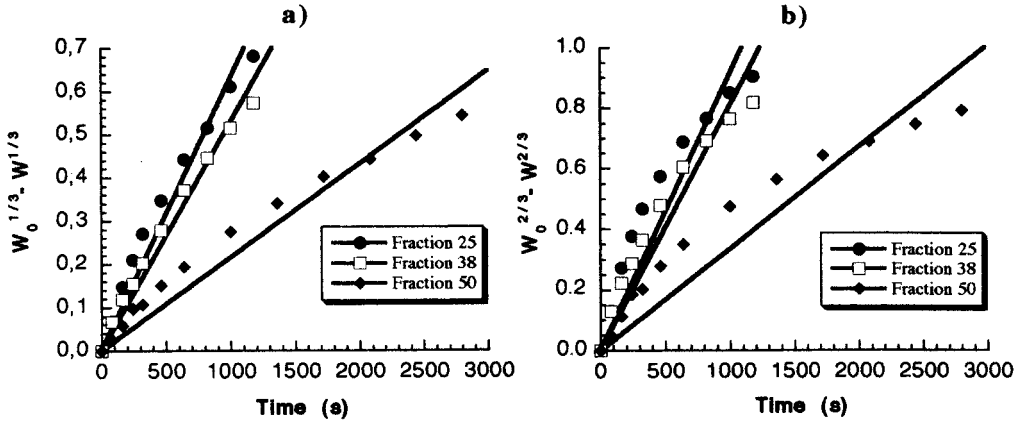


**Figure 4**—Application of the (a) Hixson–Crowell model (eq 2) and the (b) Higuchi-Hiestand model (eq 3) to the experimental dissolution profiles.

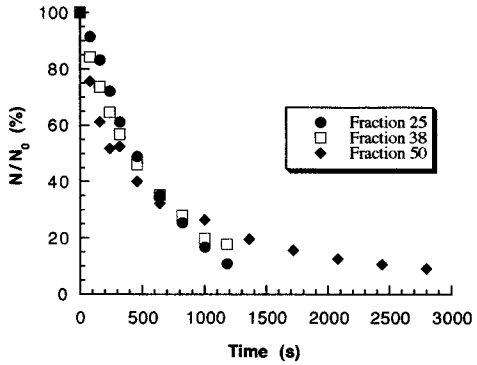


**Figure 5**—Particle number variation during dissolution expressed as a percentage of the initial number ($N_0$).

simulated and the experimental profiles, these did not exactly overlap (data not shown). That could only be achieved using another value of $k$. The best fit (quantified by the mean residue, $\bar{R}$, and maximum residue, $R_{max}$[29]) gave a value $k = 0.28$ (Figure 7), which corresponds to a value of $h$ that is approximately half of the particle radius. Values of $k$ different from 0.5 were also reported by Mauger *et al.*[13] for the dissolution of particles of prednisolone acetate. It should be outlined, however, that the exact value of $k$ is normally unknown.

Nevertheless, when a value of $k = 0.28$ was used to simulate the kinetics release of the other fractions, a discrepancy was noticed for the coarsest fraction, as illustrated in Figure 7. A good agreement was only obtained when introducing the condition that, whenever the particle size reached some critical value ($d_{crit}$), $h$ would remain constant ($=kd_{crit}$) and eq 7 should be used instead of eq 6 (see flowchart, Figure 1). A large agreement was, then, obtained for all fractions as Figure 8 shows, with $d_{crit} = 22\ \mu$m and $k = 0.26$ (quite close to the previous value). Furthermore, the fact of these agreements are observed over the entire dissolution profile substantiates the reliability of the above assumptions.

Since no more samples of ibuprofen were available, and in order to test the capability of the program to predict the dissolution profiles of broader distributions (which seems to be a major cause for the lack of fit), additional experiments were carried out using mixtures of the finest and coarsest fractions. As can be seen from Figure 9, equally good fittings were obtained, which confirms the adequacy of the model to predict dissolution profiles based only on the primary particle size distributions (once the drug characteristics are known).

## Conclusions

This study has demonstrated that the main reason for the inadequacy of the classical dissolution models to predict the release kinetics of the ibuprofen fractions is due to the assumptions associated with these models not being valid for the case of multisized powders. This conclusion was made possible by the Coulter Multisizer, which counts and sizes the suspended particles as a function of time. Furthermore, the utilization of the Coulter Multisizer for dissolution studies is extremely convenient since, with a single technique, it is possible to obtain the number and size distribution of the particles in suspension at any instant and, simultaneously, to determine the absolute concentration of the solids. The drug dissolution profile can be easily evaluated from the latter.

Thus, it was possible to prove that the number of particles in suspension continuously diminishes as dissolution proceeds, contrary to the constant value assumed by the models.

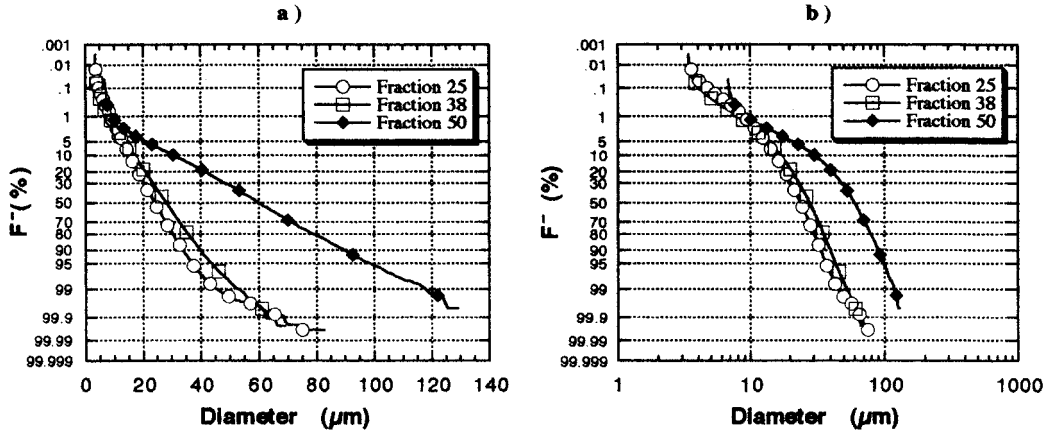


**Figure 6**—Mass cumulative size distributions of the primary ibuprofen fractions plotted on (a) log–normal and (b) normal probability paper.

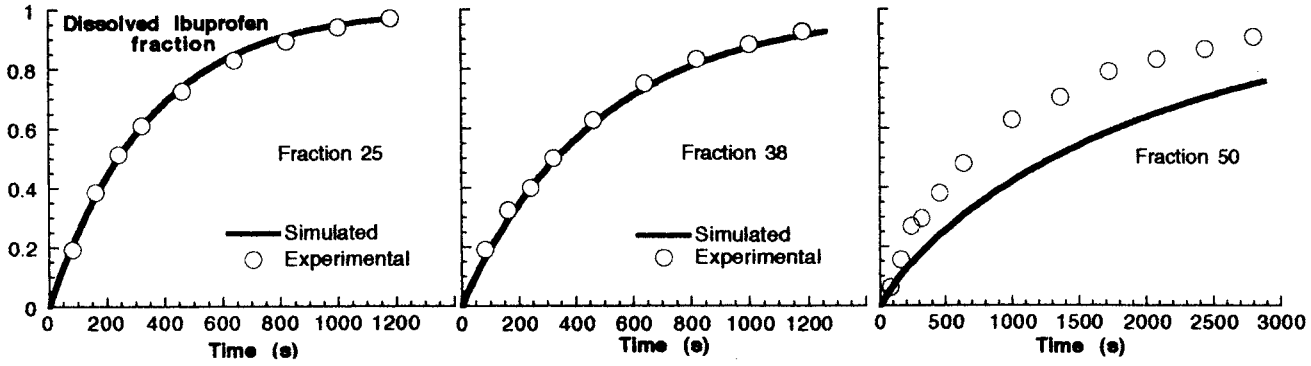


**Figure 7**—Experimental *versus* simulated ($k = 0.28$) dissolution profiles of the various ibuprofen fractions: fraction 25, $\bar{R} = 0.012$ and $R_{max} = 0.021$[29]; fraction 38, $\bar{R} = 0.016$ and $R_{max} = 0.034$; fraction 50, $\bar{R} = 0.142$ and $R_{max} = 0.206$.

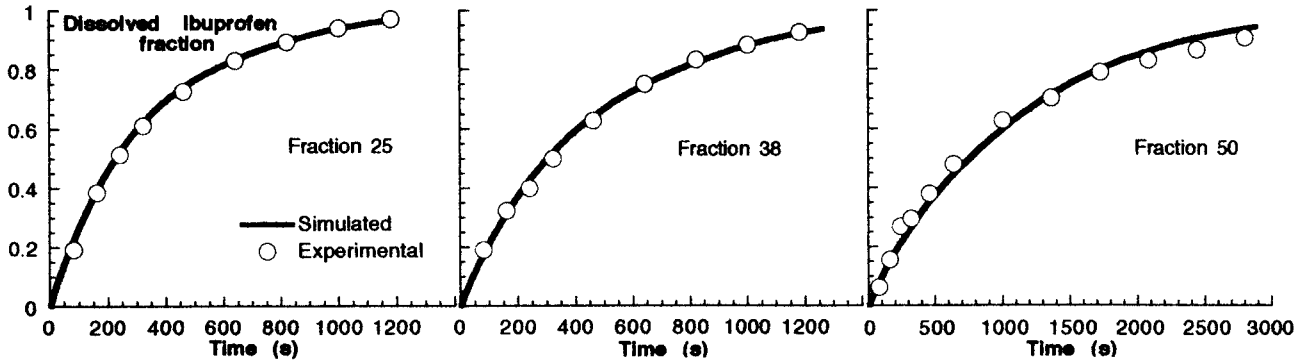


**Figure 8**—Experimental *versus* simulated ($k = 0.26$, $d_{crit}$=*22* $\mu$m) dissolution profiles of the various ibuprofen fractions: fraction 25, $\bar{R} = 0.009^{29}$ and $R_{max} = 0.029$; fraction 38, $\bar{R} = 0.011$ and $R_{max} = 0.028$; fraction 50, $\bar{R} = 0.024$ and $R_{max} = 0.040$.

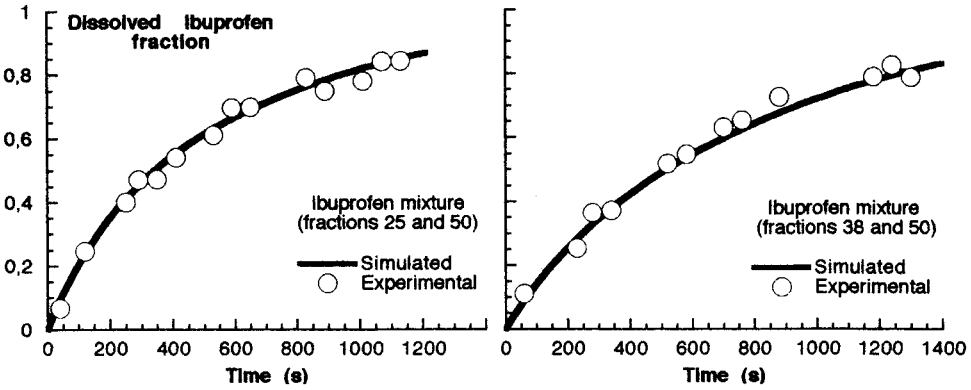


**Figure 9**—Experimental *versus* simulated ($k = 0.26$, and $d_{crit}$=*22* $\mu$m) dissolution profiles of mixtures of two ibuprofen fractions (weight ratios of 1:1): mixture of fraction 25/fraction 50, $\bar{R} = 0.020^{29}$ and $R_{max} = 0.041$; mixture of fraction 38/fraction 50, $\bar{R} = 0.025$ and $R_{max} = 0.050$.

Besides, it was apparent from the measured size distributions (and despite the analyzed fractions being relatively narrow) that these were far from monodisperse, another of the conditions assumed by the classical models.

The strategy adopted in this work was to divide the primary particle size distribution of the fraction under study into a large number of size classes, so that the particles in each class could be considered monodisperse. A dissolution kinetics equation was then applied to every class, and the calculated dissolution profiles compared to those obtained experimentally. This procedure enabled the choice of the most adequate dissolution law.

Although previous studies had indicated that the equations based on a size dependent diffusion layer thickness would be more adequate, it was found out that a single dissolution equation was not able to describe the release profiles for all the size ranges tested. As a matter of fact, the use of a constant diffusion layer model, above a given particle size, greatly improved the fitting between the model and the experimental data for the coarsest fraction. Both the proportionality constant between the boundary layer thickness and particle size ($k$) and the critical particle diameter ($d_{crit}$) were optimized from the experimental dissolution profiles. The remarkably good agreements between the simulated and the experimental data over the entire dissolution profile, for all size fractions, suggest that the assumptions made are physically realistic.

In conclusion, the methodology now proposed to predict the dissolution of ibuprofen has proved to be accurate and mathematically straightforward, requiring, basically, the primary characteristics of the powdered drug. Additionally, the use of the real particle size distribution and shape factor represents a great advantage over the procedures which assume these parameters. Indeed, nowadays, with so many accessible sizing techniques, there is no need to approximate the drug particle size distribution to a predetermined law.

In summary, it is believed that this approach is most promising to predict dissolution profiles, its strongest point being the fact that it could eventually be applicable to virtually all multisized powder drugs. Further experiments with other sparingly soluble drugs are necessary to demonstrate its general applicability.

## References and Notes


1. Abdou, H. M. In *Dissolution Bioavailability & Bioequivalence*; Mack Publishing Co.: Easton, PA, 1989.
2. Martin, A.; Swarbrick, J.; Cammarata, A. In *Physical Pharmacy. Physical Chemical Principles in the Pharmaceutical Sciences*; Lea & Febiger: Philadelphia, 1983.
3. Ford, J. L. In *Encyclopedia of Pharmaceutical Technology*; Swarbrick, J., Boylan, J. C., Eds.; Marcel Dekker: New York, 1991; Vol. 4, pp 121−167.
4. Stout, P. J.; Howard, S. A.; Mauger, J. W. In *Encyclopedia of Pharmaceutical Technology*; Swarbrick, J., Boylan, J. C., Eds.; Marcel Dekker: New York, 1991; Vol. 4, pp 169−192.
5. Simões, S.; Sousa, A.; Figueiredo, M. *Int. J. Pharm.* **1996**, *127*, 283− 291.
6. Simões, S.; Pereira de Almeida, L.; Figueiredo, M. *Int. J. Pharm.* **1996**, *139*, 169−176.
7. Noyes, A. A.; Whitney, W. R. *J. Am. Chem. Soc.* **1897**, *19*, 930−934.
8. Nernst W. *Z. Phys. Chem.* **1904**, *47*, 52−55.
9. Brunner, E. *Z. Phys. Chem.* **1904**, *47*, 56−71.
10. Hixson, A. W.; Crowell, J. H. *Ind. Eng. Chem.* **1931**, *23*, 923−31.
11. Higuchi, W. I.; Hiestand, E. N. *J. Pharm. Sci.* **1963**, *52*, 67−71.
12. Niebergall, P. J. Milosovich, G.; Goyan, J. E. *J. Pharm. Sci.* **1963**, *52*, 236−41.
13. Mauger, J. W.; Howard, S. A.; Amin, K. *J. Pharm. Sci.* **1983**, *72*, 190−193.
14. Hintz, R. J.; Johnson, K. C. *Int. J. Pharm.* **1989**, *51*, 9−17.

15. Lu, A. T. K.; Frisella, M. E.; Johnson, K. C. *Pharm. Res.* **1993**, *10*, 1308−1314.
16. Carstensen, J. T.; Musa, M. N. *J. Pharm. Sci.* **1972**, *61*, 223−226.
17. D. Brooke. *J. Pharm. Sci.* **1973**, *62*, 795−798.
18. Pedersen, P. V.; Brown, K. F. *J. Pharm. Sci.* **1975**, *64*, 1192−1195.
19. Anderberg, E. K.; Nyström, C. *Int. J. Pharm.* **1990**, *62*, 143−151.
20. Allen, T. In *Particle Size Measurements*, 4th ed.; Chapman and Hall: London, 1990.
21. Lines, R. W. In *Particle Size Analysis*.; Stanley-Wood, Lines, R. W., Eds.; Royal Society of Chemistry: London, 1992; pp 350−373.
22. Nyström, C.; Mazurt, J.; Barnett, M. I.; Glazer, M. *J. Pharm. Pharmacol.* **1985**, *37*, 217−221.
23. BS 3406, *British Standards Institution* Part 5, 1983.
24. Bernard, J. G.; Jansma, H. L.; Merkus, H. G.; Scarlett, B. In *Particle Size Anaysis*; Lloyd, P. J., Ed.; John Wiley & Sons: London, 1988; pp 135−149.
25. Alderborn, G.; Nyström, C. In *Industrial Aspects of Pharmaceutics*; E. Sandell, Ed.; Swedish Pharmaceutical Press: Sweden, 1993.
26. Lowell, S.; Shields, J. E. In *Powder surface area and porosity*, 2nd ed.; Powder Technology Series; Chapman Hall: London, 1984.
27. Levich, V. G. In *Physico-chemical Hydrodynamics*; Prentice Hall: Englewood Cliffs, NJ, 1962.
28. Council of Europe. *European Pharmacopeia*; Sainte-Ruffine: Maissonneuve S. A., 1986; V 5.4.
29. The mean and maximum residues were calculated according to the following expressions:

$$\text{mean residue} = \bar{R} = \frac{1}{n}\sum\frac{1}{w_0}\sqrt{(w_{\exp_j} - w_{\sim_j})^2} \qquad j = 1, \ldots, n$$

where $n$ = number of experimental points, $w_0$ = initial solids weight, $w_{\exp_j}$ = experimentally determined weight of solids at time $j$, and $w_{\sim_j}$ = simulated weight of solids at time $j$, and

$$\text{maximum residue} = R\max = \max\{\sqrt{(w_{\exp_j} - w_{\sim_j})^2}\} \qquad j = 1, \ldots, n$$

## Acknowledgments

The authors are most grateful to Boots Pharmaceuticals for having offered the ibuprofen samples.

JS960417W